High-Resolution Spectroscopic Diagnostics of the Hot Plasma in the Stellar Wind of ε Canis Majoris (B2 II)

David H. Cohen, Stanley P. Owocki, Joseph P. Cassinelli, & Joseph J. MacFarlane

1. Introduction

Soft X-ray emission is the most direct observational diagnostic of the time-dependent, chaotic structure in the shocked winds of hot stars. OB stars are characterized by fast line-driven winds, and our understanding of the mean, time-averaged properties of these outflows is quite advanced. Indeed, the underlying time-*independent* (CAK[1]) theory has now been extended to line-driven outflows from AGNs, novae, and disks. However, it is well known that line-driving is subject to an inherent instability[2,3], which leads to highly time-dependent structure, shocks, and the production of X-rays. High resolution X-ray spectroscopy is vital for determining in what part of the wind the X-rays are produced, for quantifying the shock strength distributions and the time-variability of the X-ray production mechanism, and ultimately for understanding basic physics of the instability itself. Due to its combination of good spectral resolution and high throughput, *XMM* provides a unique opportunity for answering several outstanding questions about shocks in hot star winds. The understanding of the line-force instability gained by *XMM* spectroscopy of hot stars can then be applied to the more exotic objects in which line-driven outflows occur.

By diagnosing the density, temperature, and spatial distribution of the shocked plasma, *XMM* can answer the fundamental question: Are wind shocks formed from self-excited instabilities or are clump-clump collisions caused by perturbations at the base of the outflow responsible? Numerical modeling of the line-driving instability has indicated that the winds of hot stars should be dominated by reverse shocks, in which low density, rapidly accelerated material impacts denser, slower moving clumps[4,5]. This basic mechanism, in which the instability is self-excited (i.e. without any initial seed perturbation), cannot, in general, reproduce the high levels of X-ray emission observed in O stars, as only a very small fraction of the stellar wind is predicted to be shock-heated at any given instant. This deficiency is not as great for early-B stars, which have lower X-ray luminosities. However, it has recently been shown that with low-level stochastic perturbations at the base of the wind, the dense clumps initially formed by the instability may interact strongly with each other further out in the wind flow, leading to shocked regions with much higher densities than can be produced by self-excited instabilities[6]. In Fig. 1 we show a representative result from our numerical simulations of instability-generated structure in the wind of ε CMa.

Another outstanding question that *XMM* can address is the surprising lack of X-ray time-variability seen in hot stars. This current broadband X-ray constraints (from e.g. *ROSAT*) imply that there may be numerous shock interaction regions, each of which subtend only a small solid angle[7]. Here again, time-resolved high-resolution X-ray spectroscopy is crucial for determining—via measurements of time-variability of individual spectral features—the number of different physical sites of X-ray production in these winds.

Finally, there are several lines of evidence[7,8,9,10] that, in at least some hot stars, the line-force instability mechanism is augmented by other mechanisms, perhaps related to magnetic fields or non-thermal emission from inverse-compton scattering of photospheric UV radiation on shock-accelerated relativistic electrons in the wind. Quantitative spectroscopic diagnostics—of temperature distributions, densities, and physical locations relative to the stellar surface—can provide information about the nature of these additional mechanisms that may enhance the ability of the line-force instability to produce X-ray emitting plasma. For example, *ASCA* observations of ε CMa[11] show a hard tail that may be indicative of the presence of some plasma with temperatures greater than 10 million K—hotter than predicted from simulations of the line-force instability. *RGS* data in second order and *EPIC* data will be able to put much tighter constraints on the nature of this harder emission and the properties of the plasma from which it emanates.

2. ε Canis Majoris

There are several reasons the B bright giant ε CMa makes an ideal laboratory for the study of the line-force instability, wind shocks, and their associated X-ray emission. First, the filling factor of hot gas in the wind is such that the self-excited instability cannot immediately be ruled out as the primary X-ray production mechanism[12], although clump-clump collisions cannot be ruled out either. Second, the wind density is low enough that X-rays produced relatively close to the stellar photosphere can be observed, yet a modest amount of wind attenuation of X-rays does exist. This wind attenuation is an important diagnostic, as we will further discuss below. And third, because it lies in an evacuated interstellar tunnel, ε CMa is the *only* early-type star for which EUV spectroscopic data is available below 504 Å. These *Extreme Ultraviolet Explorer* (*EUVE*) data (which we show in Fig. 2), have at least five emission lines of iron (from Fe IX to Fe XVI) at resolution, $R \equiv \lambda/\Delta\lambda \approx 300$[12,13]. When combined with this *EUVE* data, the *XMM* spectroscopy will provide the most stringent observational constraints of the hot plasma properties available for any hot star.

With a V-magnitude of 2, ε CMa is one of the most well-studied early-type stars, with high quality observations in every wavelength band from X-ray to IR. It shows weak wind-broadened UV absorption profiles[14], with maximum blue edge velocities of 700 km s^{-1} and a mass-loss rate that is predicted to be 10^{-7} M_{sun} yr^{-1}, but with a large amount of observational uncertainty. Previous X-ray observations made with the *ROSAT PSPC* show a normal soft spectral energy distribution and $L_x/L_{bol} \sim 10^{-7}$, with no evidence for short-term, broad-band variability above roughly 10%[15]. These X-ray properties are typical of hot stars.

By combining the *ROSAT PSPC* data with the *EUVE* spectra, we were able to show that there is a continuous distribution of plasma temperatures, up to roughly 7 million degrees K, but which is weighted toward cooler temperatures[12] (and with the possibility of some still hotter plasma, as indicated by *ASCA SIS* measurements discussed above). The *EUVE* and *ROSAT* data also were used to verify the presence of wind attenuation of the soft X-ray and, especially, the *EUVE* emission[12]. When this analysis was combined with modeling of the He II 304 Å and O III 374 Å lines measured with EUVE, a coherent picture emerges. X-rays that are spatially distributed throughout the flow are reprocessed—via the ionization and subsequent recombination cascade of helium in the cool, unshocked portion of the wind—into He II Lyman-α emission, and then via the Bowen mechanism into O III emission[13,16]. This picture of a pervasive X-ray radiation field, which is both a product of the time-dependent wind dynamics and a cause of the thermal and ionization conditions in the bulk stellar wind, can be further elucidated by spectroscopic measurements made with the *XMM RGS*. In the next section, we discuss specific spectral diagnostics, and relate them to the underlying plasma conditions and wind physics.

3. XMM Spectral Diagnostics of Hot Star Winds

Because of the combination of high spectral resolution and high throughput available for the first time with the *XMM RGS*, there are several different new spectral diagnostics which we will employ in order to address outstanding questions about the X-ray emission from ε CMa and from hot star winds in general. These are summarized in Table 1, and include consideration of photoionized cold plasma as well as thermal and non-thermal emission from hot plasma[17].

XMM Spectral Diagnostic	Plasma Property	Physical Process/Wind Property
He-like to H-like intensity ratios Iron L-shell line ratios	Electron temperature	Shock-strength distribution; nature of post-shock cooling regions; presence of non-shock heating mechanisms
He-like FIR line ratios (esp. O and Ne; see Fig. 3)	Electron density	Compression factor of shocks; physical location in the wind of shocked zones
Bound-free continuum absorption (attenuation of the spectrum in general, but also can lead to blue-red asymmetry in wind-broadened line-profiles)	Column density of material above shocked zones	Physical location of wind shocks
K-shell edge decrements and inner-shell bound-bound absorption (primarily oxygen)	Ionization balance; column density of material above shocked zones	Ionization conditions in ambient wind; physical location of shocked zones
Continuum emission intensity (above 1 keV)	Relative contribution of free-free and inverse Compton processes	Presence of Fermi-accelerated fast electrons; metal abundance; radiation transfer effects
Line widths (even a simple *detection* of wind-broadening would be unprecedented)	Bulk velocities	Physical location in the wind of the sites of X-ray emission
Time variability of emission lines and line ratios	Variability of temperature/density distributions in the X-ray emitting plasma	Variability in the X-ray production efficiency of shocks; estimate of the number of different shocked zones in the wind

Very few of these hot-star wind diagnostics have been available previously, and none with the degree of quantitative detail that will be provided by the reflection grating spectrometer aboard XMM. In fact, along with AXAF[*], XMM gives us the first opportunity to employ for astrophysical plasmas spectral diagnostics of the type

[*] ε CMa is neither a GTO nor a AO-1 GO AXAF target.

used by physicists studying hot plasmas in the laboratory (see for example Ref. 18). We provide further details of several of these diagnostics in the figure captions on the final page.

Plan for Data Analysis

Data with the quality and complexity of *XMM RGS* spectra will require much more than off-the shelf models if we are to derive the maximum amount of information about the highly structured, shocked wind of ε CMa. Our group of investigators has a great deal of expertise in all the important areas: data reduction and analysis, atomic and spectral modeling, and numerical modeling.

Cassinelli has been involved in X-ray observations of hot stars since his initial predictions of Auger ionization in hot star winds and subsequent *EINSTEIN SSS* observations[19]. Owocki has led much of the development of numerical models of time-dependent line-driven winds[3,20]. Cohen has constructed detailed models of X-ray emission to fit EUV and X-ray spectra[7,12]. MacFarlane has developed non-LTE (collisional-radiative equilibrium) models of wind excitation/ionization to model the effect of X-rays on bulk wind properties[21] and also to model the Bowen fluorescence mechanism in ε CMa[16]. Both Cohen and MacFarlane have used high-resolution X-ray spectroscopy to study hot plasmas in the laboratory, including inner-shell ionization[22] which is central to several of the diagnostics we plan to employ with the *RGS* data.

We have several modeling tools to bring to bear on these data. These include primarily a suite of atomic and collisional-radiative codes for modeling the detailed excitation dynamics in the wind and synthesizing X-ray spectra[23], and a radiation-hydrodynamics code for modeling the line-force instability[4].

Technical Considerations

We have studied this star extensively with *EUVE*, *ROSAT*, and *ASCA* and so its flux, and to some extent its spectral energy distribution, is known. Using PIMMS, we find an expected RGS count rate of 0.19 in first order and 0.02 in second order. The star is in a very uncrowded X-ray field, and the only contamination we need to be concerned about is from a 4th magnitude M star, σ CMa, at a distance of a little more than a degree. We have used SciSim to determine the position angle constraint. Because of its optical/UV brightness, the OM will not be employed for our observations. We request a 40 ksec observation based on spectral modeling we have performed with XSPEC and the RGS response matrices. A first order spectrum generated in 40 ksec will contain 7 lines with more than 100 counts and an additional 10 lines with 50 counts or more. Several more lines with between 50 and 125 counts will be seen in the second order spectrum. Lines with more than 100 counts will have a signal-to-noise ratio sufficient to allow us to perform time variability analysis.

References

1. Castor, J.I., Abbott, D.C., & Klein, R.I. 1975, *Ap.J.*, **195**, 157 (CAK)
2. Milne, E.A. 1926, *MNRAS*, **86**, 459
3. Lucy, L.B., & Solomon, P.M. 1970, *Ap.J.*, **159**, 879
4. Cooper, R.G., & Owocki, S.P. 1994, *Ap&SS*, **221**, 427
5. Feldmeier, A. 1995, *A&A*, **299**, 523
6. Feldmeier, A., Puls, J., & Pauldrach, A.W.A. 1997, *A&A*, **322**, 878
7. Cohen, D.H., Cassinelli, J.P., & MacFarlane, J.J. 1997, *Ap.J.*, **487**, 867
8. Cohen, D.H., Cassinelli, J.P., & Waldron, W.L. 1977, Ap.J., **488**, 397
9. Schmitt, J.H.M.M., Zinnecker, H., Cruddace, R., & Harnden, F.R. 1993, *Ap.J.*, **402**, L13
10. Chen, W., & White, R. 1991, *Ap.J.*, **366**, 512
11. Cohen, D.H., & Cassinelli, J.P. 1999, in preparation
12. Cohen, D.H., Cooper, R.G., MacFarlane, J.J., Owocki, S.P., Cassinelli, J.P., & Wang, P. 1996, *Ap.J.*, **460**, 506
13. Cassinelli, J.P., et al. 1995, *Ap.J.*, **438**, 932
14. Snow, T.P., & Morton, D.C. 1976, *Ap.J.S.*, **32**, 429
15. Drew, J.E., Hoare, M.G., & Denby, M. 1994, *MNRAS*, **266**, 917
16. MacFarlane, J.J., Cohen, D.H., Cassinelli, J.P., & Wang, P. 1996, in *Astrophysics in the Extreme Ultraviolet*, eds. Bowyer & Malina, (Kluwer: Dordrecht), p. 375
17. Paerels, F., et al. 1998, *High Resolution Spectroscopy with XMM*, 1st *XMM* conference
18. Goldstein, W. 1993, in *UV and X-ray Spectroscopy of Astrophysical and Laboratory Plasmas*, eds. Silver & Kahn, (Cambridge University Press: Cambridge), p. 15
19. Cassinelli, J.P., & Swank, J.H. 1983, *Ap.J.*, **271**, 681
20. Owocki, S.P., & Puls, J. 1996, *Ap.J.*, **462**, 894
21. MacFarlane, J.J., Cohen, D.H., & Wang, P. 1994, *Ap.J.*, **437**, 351
22. MacFalane, J.J., Wang, P., Bailey, J.E., Mehlhorn, T.A., & Dukart, R.J. 1995, *Laser & Part. Beams*, **13**, 231
23. MacFarlane, J.J. 1997, UWFDM, fti.neep.wisc.edu/FTI/pdf/fdm1050.pdf
24. Linsky, J.L., & Gagne, M. 1998, in *The Tenth Cambridge Workshop on Cool Stars, Stellar Systems and the Sun*, eds. Donahue & Bookbinder, (ASP Conf. Series), p.527

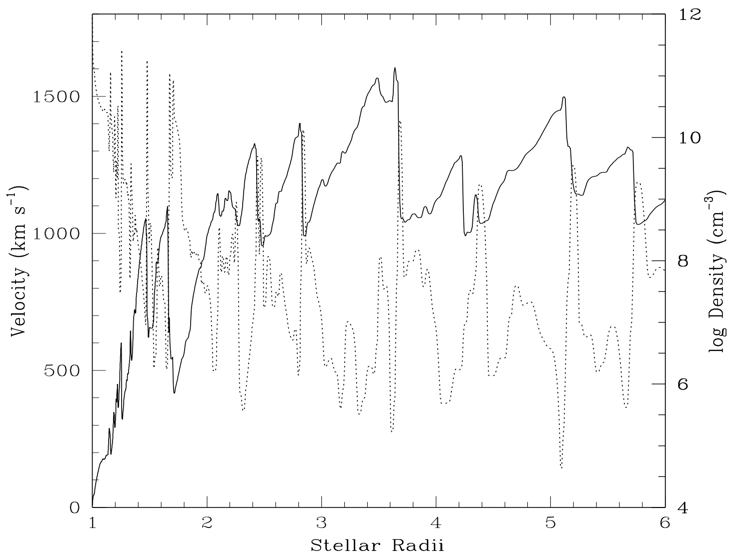

Figure 1 (above) — Velocity- (solid) and density-profiles (dotted) from a numerical simulation of self-excited structure in the unstable wind of ε CMa. Note that the material flowing into shocks tends to be low density—this is not the case for clump-clump collisions. There are issues of lower boundary conditions, as well as features like rotation and star spots (in our 2-D models) and magnetic fields that can be tested quantitatively using *XMM* data.

Figure 2 (below left) — *EUVE MW* spectrum of ε CMa. Note the highly-ionized iron lines, which are formed in plasma with temperatures ranging from 0.5 million K (Fe^{+8}) to 3 million K (Fe^{+15}). Also note the He II and O III lines which are formed in the cold, unshocked wind, but are sensitive to the level of soft-X-ray emission in the shocked wind.

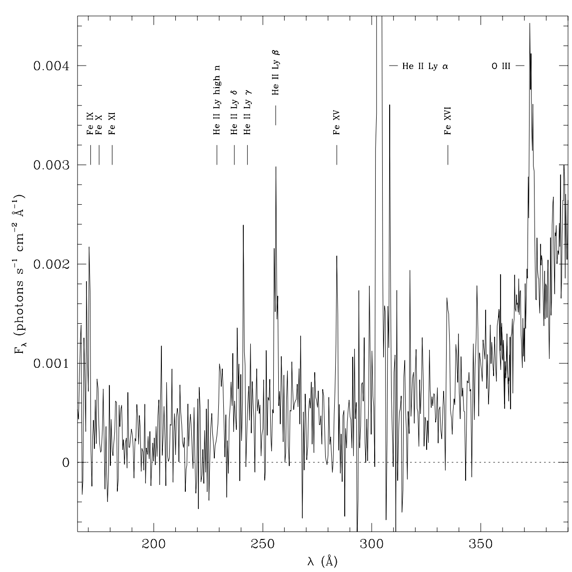

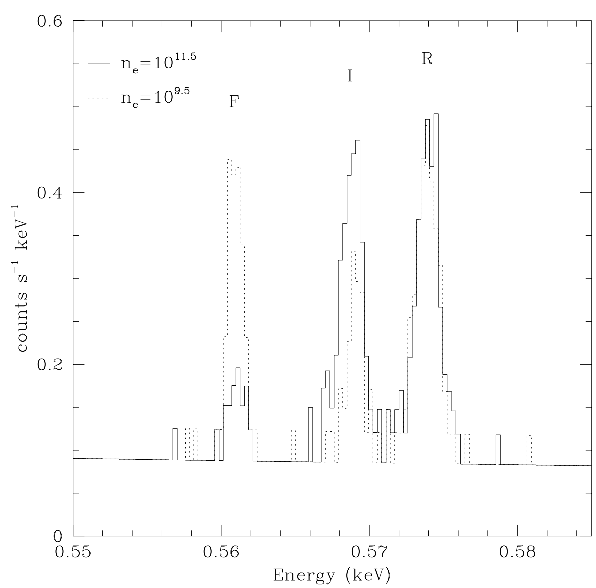

Figure 3 (above right) — Density sensitive "FIR" lines from He-like oxygen in a 40 ksec simulation of ε CMa. Because of collisional quenching of the forbidden line above a critical density of n_e=$10^{10.7}$ cm^{-3} for oxygen, the F/I line intensity ratio can be used to discriminate densities[24]. For He-like O, the critical density is close to what would be expected in the shock zones produced by clump-clump collisions. If self-excited instabilities dominate the shock structure in the wind of ε CMa, then the densities will be below the critical density, and the forbidden line will not be quenched. Higher density, hotter plasma will be probed with the neon F/I intensity ratio, seen in the second order RGS spectrum. Note that our requested 40 ksec exposure will give approximately 250 counts in the O VII resonance line.